



HAL
open science

The MOX Powder Calculation Challenge OECD Benchmark Proposal and CRISTAL-RIB Results

A. Santamarina, C. Riffard

► **To cite this version:**

A. Santamarina, C. Riffard. The MOX Powder Calculation Challenge OECD Benchmark Proposal and CRISTAL-RIB Results. ICNC 2015 - International Conference on Nuclear Criticality, Sep 2015, Charlotte, United States. cea-02489557

HAL Id: cea-02489557

<https://cea.hal.science/cea-02489557v1>

Submitted on 30 Mar 2020

HAL is a multi-disciplinary open access archive for the deposit and dissemination of scientific research documents, whether they are published or not. The documents may come from teaching and research institutions in France or abroad, or from public or private research centers.

L'archive ouverte pluridisciplinaire **HAL**, est destinée au dépôt et à la diffusion de documents scientifiques de niveau recherche, publiés ou non, émanant des établissements d'enseignement et de recherche français ou étrangers, des laboratoires publics ou privés.

MOX POWDER CALCULATION IMPROVEMENT: OECD BENCHMARK PROPOSAL AND CRISTAL-RIB RESULTS

A. Santamarina and C. Riffard

Commissariat à l'Énergie Atomique et aux Énergies Alternatives
CEA, DEN, DER, SPRC, Cadarache
F-13108 Saint-Paul-Lez-Durance, France.
alain.santamarina@cea.fr

ABSTRACT

In the framework of the WPNCs Expert Group on Uncertainty Analysis for Criticality Safety Assessment, we propose a blind numerical benchmark. Since the WPNCs Expert Group on Experimental Needs had highlighted the poor database of representative experiments of low-moderated MOX powders, this blind benchmark is focused on MOX wet powders. Three PuO₂ contents are proposed: 100%, 30% and 12.5%. Two Pu isotopic vectors are considered: a conservative one (0%, 71%, 17%, 11%, 1% for ²³⁸Pu up to ²⁴²Pu) and a realistic one obtained from reprocessed LWR 30 GWd/T fuels. For these 6 cases the powder moisture rate is 3%. The MOX fissile medium is a sphere surrounded by 20 cm water reflector. The required results are the calculated K_{eff} and the associated prior uncertainty. Using benchmark experiments, contributors should provide the projected-K_{eff} and the corresponding posterior uncertainty. CRISTAL-V2 results based on JEFF3.1.1 nuclear data are presented. As an example, in the 30% PuO₂ challenging case, the calculation uncertainty is decreased from 1160 pcm (1σ) down to 450 pcm using EOLE and MASURCA critical Pu experiments. This uncertainty depends slightly on 'conservative' or 'realistic' Pu because the representativity factor does not vary significantly with the Pu vector.

KEYWORDS

UACSA, Safety-Criticality, MOX powders, blind benchmark

1. INTRODUCTION

The Pu recycle from reprocessing plants, such as La Hague in France, through MOX assemblies introduced in commercial Light Water Reactors (LWR) and future GEN-4 reactors, has emphasized the need for experimental benchmarks dealing with MOX fuel [1]. Experiments are required for criticality-safety evaluation of fuel cycle facilities, particularly MOX assembly factories. The assessment of the available benchmarks, performed by the OECD Working Party on Nuclear Criticality Safety (WPNCs) Expert Group on Experimental Needs, had highlighted the poor database of representative experiments of low-moderated MOX powders [2] [3]. Therefore, some new targeted experiments were proposed in French [4] and Russian mock-up reactors, and were evaluated [5]. In 2005-2006, a series of experiments referred to as BFS/MOX was conducted at the BFS-1 experimental facility in IPPE, Russia. Nine critical configurations with heterogeneous compositions of plutonium metal, depleted uranium dioxide and polyethylene were assembled [6]. However, the strong heterogeneity of these experiments raised a representativity problem compared to homogeneous MOX powders, as well as some calculation difficulties in the analysis.

Furthermore, the WPNCs Expert Group on Uncertainty Analysis for Criticality Safety Assessment (UACSA) was created in December 2007 to assess calculation uncertainty in Criticality Safety studies.

Exercise Phase I was conducted in order to illustrate predictive capabilities of criticality validation approaches, which include similarity assessment, selection of relevant experiments, determination of k_{eff} bias and bias uncertainty [7]. Unfortunately, this numerical benchmark proposed application cases corresponding to experimental benchmarks of the OECD Experiment data base IHECSBE [8] : thus the projected calculated eigenvalue is known ($K_{eff}=1$), that limits the actual spread among contributor results.

Therefore, in the framework of the UACSA Expert Group, we propose a numerical blind benchmark. Due to the challenging calculation of Pu resonant reaction rates in intermediate spectra, we have selected MOX powder applications encountered in fuel cycle facilities. This new benchmark should allow the evaluation of the ability of validation methods based on mock-up experiments to determine the Bias on the predicted k_{eff} and the corresponding bias Uncertainty.

2. BLIND BENCHMARK ON MOX POWDERS

Three PuO₂ contents are proposed : 100%, 30% (maximum PuO₂ load in GEN4-SFR) and 12.5% (maximum PuO₂ content in LWR-MOX pellets). The corresponding dry MOX powder density is respectively: $\rho^{MOX} = 3.5, 5.5$ and 4.6 g/cm^3 .

Two Pu isotopic vectors are considered:

- 71%, 17%, 11%, 1% for ²³⁹Pu up to ²⁴²Pu, corresponding to a conservative Pu vector..
- 64%, 23%, 10%, 3%, corresponding to a realistic Pu vector obtained from reprocessed LWR 30 GWd/T fuels. ²³⁸Pu and ²⁴¹Am poison concentrations are neglected to increase conservatism.

Concerning, the UO₂ powder, a conservative uranium isotopic enrichment is set to 1.2%.

For these 6 cases the powder moisture rate is $M_{H_2O} / (M_{H_2O} + M_{UO_2-PuO_2}) = 3\%$.

The MOX medium is a sphere, surrounded by 20 cm water reflector. The fixed radius of the 6 spheres is:
 $R_{MOX} = 17.0 \text{ cm}, 22.5 \text{ cm}, 46.0 \text{ cm}$ respectively for the 100%, 30%, 12.5%PuO₂ cases with the conservative Pu.

$R_{MOX} = 17.7 \text{ cm}, 24.1 \text{ cm}, 52.5 \text{ cm}$ respectively for the 100%, 30%, 12.5% PuO₂ cases with the realistic Pu vector.

These quasi-critical radii were assessed using CRISTAL-V2 [9] calculations based on the JEFF3.1.1 Nuclear Data Library [10].

The benchmark specifications for the 6 application cases are summarized in Table I.

Table I. Specifications of the MOX wet powder benchmark (3% w/o H₂O)

| Benchmark | MOX Radius | M _{PuO2} /M _{MOX} | ²³⁹ Pu/Pu | ²⁴⁰ Pu/Pu | ²⁴¹ Pu/Pu | ²⁴² Pu/Pu |
|-----------|------------|-------------------------------------|----------------------|----------------------|----------------------|----------------------|
| Case 1 | 17.0 cm | 100% | 71% | 17% | 11% | 1% |
| Case 2 | 22.5 cm | 30% | | | | |
| Case 3 | 46.0 cm | 12.5% | | | | |
| Case 4 | 17.7 cm | 100% | 64% | 23% | 10% | 3% |
| Case 5 | 24.1 cm | 30% | | | | |
| Case 6 | 52.5 cm | 12.5% | | | | |

Atom densities for the six benchmark cases are given in Table II.

Atom densities in the surrounding water reflector are: $N_{\text{H}_2\text{O}} = 3.336\text{E-}02$ (in 10^{24} atom/cm³)

Table II. Atom densities (10^{24} atom/cm³) in the fissile spheres

| Isotope | Case 1 | Case 2 | Case 3 | Case 4 | Case 5 | Case 6 |
|-------------------|------------|------------|------------|------------|------------|------------|
| ²³⁵ U | - | 1.0434E-04 | 1.0909E-04 | - | 1.0434E-04 | 1.0909E-04 |
| ²³⁸ U | - | 8.4823E-03 | 8.8679E-03 | - | 8.4823E-03 | 8.8679E-03 |
| ²³⁹ Pu | 5.5222E-03 | 2.6033E-03 | 9.0722E-04 | 4.9800E-03 | 2.3475E-03 | 8.1816E-04 |
| ²⁴⁰ Pu | 1.3167E-03 | 6.2073E-04 | 2.1632E-04 | 1.7863E-03 | 8.4186E-04 | 2.9337E-04 |
| ²⁴¹ Pu | 8.4844E-04 | 3.9998E-04 | 1.3939E-04 | 7.6775E-04 | 3.6198E-04 | 1.2615E-04 |
| ²⁴² Pu | 7.6812E-05 | 3.6211E-05 | 1.2619E-05 | 2.3034E-04 | 1.0859E-04 | 3.7845E-05 |
| ¹⁶ O | 1.5528E-02 | 2.4494E-02 | 2.0505E-02 | 1.5528E-02 | 2.4494E-02 | 2.0505E-02 |
| H ₂ O | 3.6180E-03 | 5.6860E-03 | 4.7560E-03 | 3.6180E-03 | 5.6860E-03 | 4.7560E-03 |

The required results for each application case are:

- 1/ a brief description of codes and Nuclear Data library used
- 2/ the calculated k_{eff}
- 3/ the one-group integrated sensitivities to multiplicity, fission, capture and scattering of each isotope
- 4/ the k_{eff} prior uncertainty
- 5/ the selected relevant experiments
- 6/ the calculation bias (thus the projected k_{eff}) and the corresponding posterior uncertainty, using experiment information.

3. CRISTAL AND RIB RESULTS

3.1. Calculation codes and nuclear data library

The benchmark calculation was carried out with the new criticality package CRISTAL-V2. The multiplication factor K_{eff} was calculated both with the deterministic route APOLLO2.8 [11] using the *SHEM-MOC* calculation scheme [12] (based on the SHEM 281-group [13]) and the reference continuous-energy Monte Carlo route TRIPOLI4 [14]. Both codes use the JEFF3.1.1 library particularly validated for safety-criticality calculations [15] and LWR calculations [16]. Associated with the CRISTAL package, the RIB code [17] allows the selection of representative experiments and Bias plus Uncertainty calculation.

3.2. K_{eff} calculation results

JEFF3.1.1-based results in Table III are consistent between deterministic and Monte-Carlo calculations.

Table III. Calculation results for the six MOX-powder cases

| K_{eff} CRISTAL | Case 1 | Case 2 | Case 3 | Case 4 | Case 5 | Case 6 |
|--------------------------|---------|---------|---------|---------|---------|---------|
| TRIPOLI4 | 0.99859 | 0.99854 | 0.99889 | 0.99778 | 1.00010 | 0.99930 |
| APOLLO2.8 | 1.00056 | 1.00019 | 1.00015 | 0.99951 | 1.00092 | 1.00000 |
| AP2 – T4 (pcm) | 197±35 | 165±11 | 126±18 | 173±36 | 82±11 | 70±29 |

3.3. Sensitivity profiles

K_{eff} sensitivity profiles to nuclear data have been obtained from the First Order Perturbation Theory implemented in APOLLO2. Sensitivity profiles to the cross sections and multiplicities were calculated on the SHEM-281g mesh. The fine mesh below 23eV in SHEM allows the fine structure calculation of the adjoint flux in the first resonances of actinides. Afterwards, the sensitivity coefficients were derived on the European JEF 15-group structure. Sensitivities to $^{239}\text{Pu}(n,f)$ data are plotted in Fig. 1 (cases 1, 2, 3) : K_{eff} of the 12.5% PuO_2 powder is highly sensitive to ^{239}Pu fission at intermediate energy (resolved resonance range), while the sensitivity becomes predominant in the fast energy range for the 100% PuO_2 .

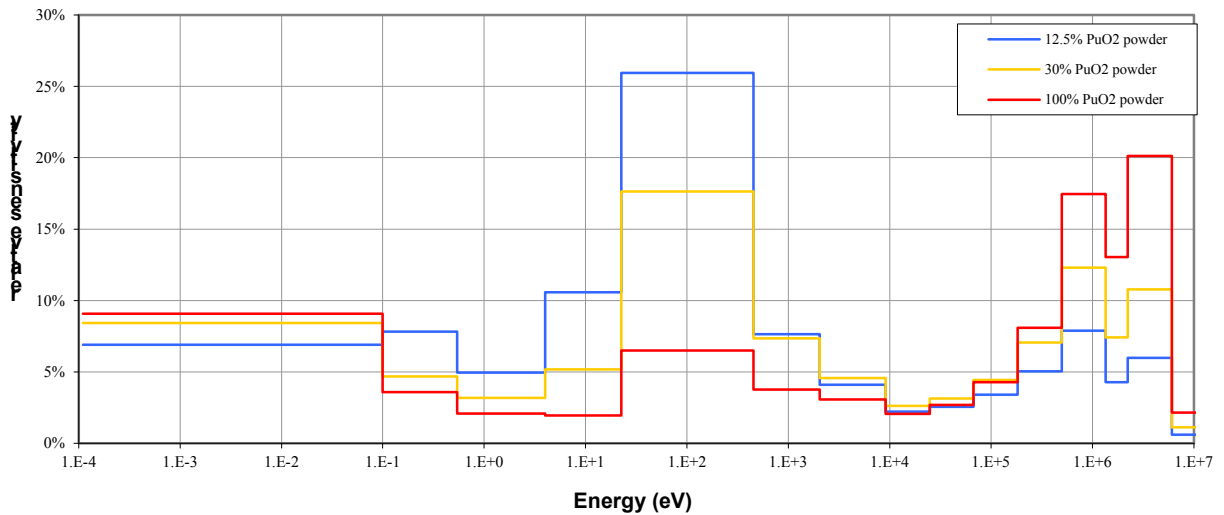


Figure 1: Sensitivity profiles to ^{239}Pu fission for MOX Applications

The integrated one-group sensitivities are summarized in Tables IV and V, respectively for the ‘conservative’ and ‘realistic’ Pu. They are quite similar for the two different isotopic vectors.

It is worth noting that JEFF3.1.1-based sensitivities in Table IV are consistent within 5% with previous JEF2-based sensitivities [18].

Table IV. Integrated sensitivity coefficients in pcm/% (cases 1, 2, 3 with conservative Pu)

| Application case | | 1: 100%PuO ₂ | 2: 30%PuO ₂ | 3: 12.5%PuO ₂ |
|------------------|---------------------------------|-------------------------|------------------------|--------------------------|
| Fission | ²³⁹ Pu | 422 | 376 | 350 |
| | ²⁴⁰ Pu | 45 | 24 | 13 |
| | ²⁴¹ Pu | 90 | 96 | 95 |
| | ²⁴² Pu | 2 | 1 | 1 |
| | ²³⁵ U | - | 12 | 33 |
| | ²³⁸ U | - | 50 | 76 |
| ν | ²³⁹ Pu | 758 | 687 | 631 |
| | ²⁴⁰ Pu | 66 | 35 | 19 |
| | ²⁴¹ Pu | 174 | 175 | 164 |
| | ²⁴² Pu | 3 | 2 | 1 |
| | ²³⁵ U | - | 24 | 63 |
| | ²³⁸ U | - | 78 | 121 |
| Capture | ²³⁹ Pu | -105 | -128 | -135 |
| | ²⁴⁰ Pu | -29 | -37 | -45 |
| | ²⁴¹ Pu | -20 | -21 | -20 |
| | ²⁴² Pu | -2 | -2 | -3 |
| | ²³⁵ U | - | -5 | -12 |
| | ²³⁸ U | - | -86 | -180 |
| | ¹⁶ O | -2 | -3 | -4 |
| | ¹ H_H ₂ O | -84 | -66 | -45 |
| Scattering | ²³⁹ Pu | 6 | 1 | -1 |
| | ²⁴⁰ Pu | 2 | 0 | 0 |
| | ²⁴¹ Pu | 1 | 0 | 0 |
| | ²⁴² Pu | 0 | 0 | 0 |
| | ²³⁵ U | - | 0 | 0 |
| | ²³⁸ U | - | 6 | -14 |
| | ¹⁶ O | 6 | 5 | -4 |
| | ¹ H_H ₂ O | 39 | 72 | 71 |

K_{eff} of the MOX powder configurations is particularly sensitive to variations of ²³⁹Pu and, to a less extent, ²⁴¹Pu nuclear data. Tables IV and V show a significant sensitivity to ²³⁸U resonant capture cross-sections, due to an intermediate neutron spectrum (demonstrated by the weak thermal slowing-down density : q_{∞} = 0.14 and 0.06 respectively for 12.5% and 30% PuO₂ powders).

Table V. Integrated sensitivity coefficients in pcm/% (cases 4, 5, 6 with realistic Pu)

| Application case | | 4: 100%PuO ₂ | 5: 30%PuO ₂ | 6: 12.5%PuO ₂ |
|------------------|---------------------------------|-------------------------|------------------------|--------------------------|
| Fission | ²³⁹ Pu | 409 | 374 | 352 |
| | ²⁴⁰ Pu | 64 | 34 | 19 |
| | ²⁴¹ Pu | 89 | 97 | 98 |
| | ²⁴² Pu | 7 | 4 | 2 |
| | ²³⁵ U | | 13 | 37 |
| | ²³⁸ U | | 52 | 79 |
| ν | ²³⁹ Pu | 728 | 667 | 613 |
| | ²⁴⁰ Pu | 93 | 50 | 28 |
| | ²⁴¹ Pu | 169 | 171 | 161 |
| | ²⁴² Pu | 10 | 5 | 3 |
| | ²³⁵ U | | 26 | 68 |
| | ²³⁸ U | | 81 | 127 |
| Capture | ²³⁹ Pu | -101 | -122 | -128 |
| | ²⁴⁰ Pu | -37 | -46 | -55 |
| | ²⁴¹ Pu | -19 | -20 | -19 |
| | ²⁴² Pu | -4 | -5 | -6 |
| | ²³⁵ U | | -5 | -13 |
| | ²³⁸ U | | -91 | -188 |
| | ¹⁶ O | -3 | -4 | -5 |
| | ¹ H_H ₂ O | -81 | -60 | -35 |
| Scattering | ²³⁹ Pu | 4 | 0 | -1 |
| | ²⁴⁰ Pu | 2 | 0 | 0 |
| | ²⁴¹ Pu | 1 | 0 | 0 |
| | ²⁴² Pu | 0 | 0 | 0 |
| | ²³⁵ U | | 0 | 0 |
| | ²³⁸ U | | 2 | -24 |
| | ¹⁶ O | 4 | 2 | -9 |
| | ¹ H_H ₂ O | 32 | 58 | 49 |

3.4. Uncertainty on nuclear data and K_{eff} prior uncertainty

The uncertainty $\varepsilon = \Delta I / I$ on a neutronic parameter I due to nuclear data is given at the first order by the “sandwich” rule [19]:

$$\varepsilon_A = \left(S_A^+ D S_A \right)^{1/2} \quad (1)$$

D: nuclear data multigroup Covariance matrix

$$S_A = \frac{\sigma^j}{I_A} \cdot \frac{dI_A}{d\sigma^j} : \text{Sensitivity vector of the Application parameter } I_A \text{ to nuclear data}$$

$S_{K_{eff}}$ sensitivity vector to nuclear data are obtained from CRISTAL calculations, as described in the previous section. Then, the K_{eff} prior uncertainty is automatically determined by the RIB code [17].

In the new CRISTAL-V2 package, the JEFF3.1.1 library is used. Covariances for this library are more reliable because they were obtained from a rigorous process : for each major actinide, the JEFF3.1.1 covariance matrix was obtained from the Nuclear Data re-estimation based on targeted experiments [20]. Prior and posterior ND Uncertainties (diagonal term of covariance matrices) are compared in Table VI. These covariance matrices are stored in the library COMAC (COvariance MATrix Cadarache [21]).

Table VI. ^{235}U Prior and Posterior uncertainty (%)

| Group/Energy | $(n,\gamma)^{\text{prior}}$ | $(n,\gamma)^{\text{post}}$ | $(n,f)^{\text{prior}}$ | $(n,f)^{\text{post}}$ | v^{prior} | v^{post} |
|------------------|-----------------------------|----------------------------|------------------------|-----------------------|--------------------|-------------------|
| Gr12 / 23-4 eV | 10 | 3.6 | 3.0 | 2.3 | 0.8 | 0.7 |
| Gr13 / 4-0.5 eV | 10 | 3.7 | 3.0 | 2.4 | 0.8 | 0.7 |
| Gr14 / 0.5-0.1eV | 2 | 1.6 | 1.0 | 0.8 | 0.8 | 0.5 |
| Gr15 / E<0.1eV | 1 | 0.8 | 0.4 | 0.3 | 0.4 | 0.2 |

The RIB results for the K_{eff} prior uncertainty are summarized in Table VII. Prior uncertainties are reduced in JEFF3.1.1-based calculations. The uncertainty level remains similar in cases characterized by either ‘conservative’ or ‘realistic’ Pu vector, due to the small uncertainty component linked to ^{242}Pu .

Table VII. Prior uncertainty (1σ) on the K_{eff} of the six fissile spheres

| Application case | 1: 100%PuO ₂ | 2: 30%PuO ₂ | 3: 12.5%PuO ₂ | 4: 100%PuO ₂ | 5: 30%PuO ₂ | 6: 12.5%PuO ₂ |
|-----------------------|----------------------------|---------------------------|-----------------------------|----------------------------|---------------------------|-----------------------------|
| JEF2 calculation | 1590 pcm | 1340 pcm | 1310 pcm | 1600 pcm | 1350 pcm | 1330 pcm |
| JEFF3.1.1 calculation | 1380 pcm | 1150 pcm | 1060 pcm | 1390 pcm | 1160 pcm | 1080 pcm |

3.5. Selected representative experiments

In order to select Experiments relevant for the industrial Application we use the Representativity r_{AE} [23] :

$$r_{AE} = \frac{(S_A^+ DS_E)}{\varepsilon_A \cdot \varepsilon_E} \quad (2)$$

This correlation coefficient r_{AE} represents the share of information provided by the experiment E common with the parameter $K_{eff,A}$. A value of 0.0 means that the Experiment and the Application are not correlated. Information provided by the experiment E will not be of any utility for the validation of the application. On the contrary, a value of 1.0 indicates a full correlation between Experiment and Application that allows a strong calculation uncertainty reduction.

In this preliminary work, only critical experiments from the French experimental database were selected:
 - The ERASME experiments [22], achieved in the EOLE facility at Cadarache in the 1984-1986 period, was built up to reduce the uncertainties on High Conversion PWR parameters. MOX 11%Pu fuel rods are

used in tight lattices ($V_{\text{mod}}/V_{\text{MOX}}$ ranging from 0.5 up to 2.1). The tightest configuration ERASME/S is available in the Experiment data base IHECSBE as MIX-COMP-INTER-005.

- The 1A' experiment has been carried out in the MASURCA facility at Cadarache in 1969: it was conceived within the framework of the Fast Breeder Reactor design. The core was constituted of U-Pu metallic fuel assemblies. The moderator was graphite.

The main characteristics of these two uncorrelated experiments are summarized in Table VIII.

Table VIII. Selected U-Pu experiments in EOLE and MASURCA reactors

| Experiment | Pu (%) | ²⁴⁰ Pu (% Pu) | Lattice pitch (cm) | Moderator | $V_{\text{mod}}/V_{\text{MOX}}$ | Slowing-down density q_{∞} | $\epsilon_{\text{exp}} (1\sigma)$ (pcm) |
|------------|--------|--------------------------|--------------------|-----------|---------------------------------|-----------------------------------|---|
| 1A' | 25 | 8.4 | □ 1.39 | Graphite | 4.1 | 0.002 | 500 |
| ERASME/S | 11 | 18.6 | △ 0.945 | Water | 0.5 | 0.28 | 400 |
| ERASME/R | | | △ 1.035 | | 0.9 | 0.42 | 400 |
| ERASME/L | | | □ 1.19 | | 2.1 | 0.66 | 310 |

△ - triangular pitch, □ - square pitch

Table IX gives respectively the Representativity factor r of these critical experiments to the various low-moderated MOX powders ('conservative' Pu vector). ERASME/S presents the highest correlation coefficient with respect to 12.5% PuO₂ powder with $r = 0.987$ while experiment 1A' is more representative of the powders with 30 and 100% PuO₂ content (respectively $r = 0.964$ and 0.929).

Table IX. Representativity factor

| Experiment | 12.5% PuO ₂ powder | 30% PuO ₂ powder | 100% PuO ₂ powder |
|------------|-------------------------------|-----------------------------|------------------------------|
| ERASME/S | 0.987 | 0.907 | 0.711 |
| ERASME/R | 0.949 | 0.866 | 0.666 |
| 1A' | 0.882 | 0.964 | 0.929 |

3.6. Calculation Bias and bias Uncertainty

Due to the same fuel pins, experiments ERASME/R and ERASME/S are strongly correlated. Therefore, only ERASME/S and 1A' experiments are taken into account in the RIB assessment of the CRISTAL-V2 calculation bias and associated posterior uncertainty.

Each measured parameter $I_{E_i} \pm \delta_i$ affects the computation parameter I_A and its posterior uncertainty accordingly to its weight w_i :

$$w_i = \frac{1}{1 + \delta_i^2 / \epsilon_{E_i}^2} \quad (3)$$

The lower its measurement uncertainty relatively to computation uncertainty, the more the experiment will influence the transposition from Experiment to Application.

When using only two experiments, the ΔI_A computation error and the posterior uncertainty ϵ_A^* due to nuclear data are obtained respectively by formula (4) and (5):

$$\frac{\Delta I_A}{\varepsilon_A} = \frac{1}{1 - \hat{r}_{1,2}^2 \cdot w_1 \cdot w_2} \left[r_{A,1} \cdot w_1 \cdot \frac{\Delta I_{E_1}}{\varepsilon_{E_1}} + r_{A,2} \cdot w_2 \cdot \frac{\Delta I_{E_2}}{\varepsilon_{E_2}} - \hat{r}_{1,2} \cdot w_1 \cdot w_2 \left(r_{A,2} \cdot \frac{\Delta I_{E_1}}{\varepsilon_{E_1}} + r_{A,1} \cdot \frac{\Delta I_{E_2}}{\varepsilon_{E_2}} \right) \right] \quad (4)$$

$$\frac{\varepsilon_A^{*2}}{\varepsilon_A^2} = 1 - \frac{1}{1 - \hat{r}_{1,2}^2 \cdot w_1 \cdot w_2} \left(r_{A,1} \cdot \sqrt{w_1} - r_{A,2} \cdot \sqrt{w_2} \right)^2 - \frac{2}{1 + \hat{r}_{1,2} \cdot \sqrt{w_1 \cdot w_2}} \cdot r_{A,1} \cdot r_{A,2} \cdot \sqrt{w_1 \cdot w_2} \quad (5)$$

with $\Delta I_E = \frac{I_E^m - I_E}{I_E}$: Calculation-Experiment bias on the measured parameter

$\hat{r}_{1,2}$: correlation coefficient between experiment 1 and experiment 2.

Correlation coefficient $\hat{r}_{1,2}$ gathers similarity between experiments ($r_{1,2}$) and technological/measurement correlation. As we choose 2 independent measurements, $\hat{r}_{1,2}$ becomes $r_{1,2}$: $\hat{r}_{ERASME,1A'} = r_{ERASME,1A'} = 0.89$.

The transposition of C/E discrepancies accordingly to (4) supplies the TRIPOLI4 calculation error for each MOX powder application. Results shown in Table X allow the conclusion that CRISTAL-V2 error of wet MOX powders is small : the scaling correction $-\Delta I_A$ ranges between -156 pcm and -422 pcm.

The posterior uncertainty derived from formula (5), associated to the projected- K_{eff} , is reduced at least by a factor 2 thanks to the selected U-Pu experiments. This uncertainty does not depend on 'conservative' or 'realistic' Pu vector because the representativity factor does not vary significantly with the Pu vector.

Table X. Prior and posterior $K_{eff} \pm 1\sigma$ of TRIPOLI4-JEFF3.1.1 calculation

| CRISTAL-V2 K_{eff} | Case 1 | Case 2 | Case 3 | Case 4 | Case 5 | Case 6 |
|-----------------------------|--------------------------|--------------------------|--------------------------|--------------------------|--------------------------|--------------------------|
| Scaling correction | -158 pcm | -251 pcm | -420 pcm | -156 pcm | -249 pcm | -422 pcm |
| Prior T4 results | 0.99859 ± 0.01380 | 0.99854 ± 0.01150 | 0.99889 ± 0.01060 | 0.99778 ± 0.01390 | 1.00010 ± 0.01160 | 0.99930 ± 0.01080 |
| Projected T4 results | 0.99701 ± 0.00721 | 0.99603 ± 0.00445 | 0.99469 ± 0.00395 | 0.99622 ± 0.00728 | 0.99761 ± 0.00447 | 0.99508 ± 0.00394 |

4. CONCLUSIONS

In the framework of the WPNCs Uncertainty expert Group, we propose a numerical blind benchmark on MOX wet powders. Three PuO₂ contents are investigated : 100%, 30% and 12.5%. Two Pu isotopic vectors are considered : a conservative one (0%, 71%, 17%, 11%, 1% for ²³⁸Pu up to ²⁴²Pu) and a realistic one obtained from reprocessed LWR 30 GWd/T fuels. For these 6 cases the powder moisture rate is 3%. The MOX fissile medium is a sphere, surrounded by 20 cm water reflector. The radius of the three quasi-critical spheres is : $R_{MOX} = 17, 22.5, 46$ cm respectively for 100%, 30%, 12.5% PuO₂ (conservative Pu).

We have presented the CRISTAL-V2 results based on the JEFF3.1.1 library. The K_{eff} prior uncertainty amounts from 1080 pcm for the 12.5%PuO₂ up to 1380 pcm for the 100%PuO₂ load. Using only EOLE and MASURCA benchmark experiments in the RIB automated tool, the projected- K_{eff} were obtained for the six application cases and the associated posterior uncertainties were reduced by about 60%. This preliminary study will be improved by the use of additional relevant experiments such as BFS/MOX.

ACKNOWLEDGMENTS

This work was supported by CEA and AREVA-NC.

REFERENCES

1. I. Duhamel, V. Rouyer, A. Santamarina, C. Venard, "Criticality calculation codes validation : Experimental needs for low-moderated MOX media," *Proc. of Workshop on the need of integral critical experiments with low-moderated MOX fuels*, Paris, 14-15 April 2004, Vol. I, pp. 55-66 (2004).
2. P. Blaise, P. Fougeras, A. Santamarina, S. Cathalau, "Integral needs for MOX powder: State of the art at CEA-Cadarache on MOX experiments," *Proc. Workshop*, Paris, 14-15 April 2004, Vol. I, pp. 191.
3. "The Need for Integral Criticality Experiments with Low-moderated MOX Fuels," *Workshop Proceedings*, 14 – 15 April 2004, ISBN 92-64-02078-0, NEA No.5668, OECD 2004.
4. P. Fouillaud, V. Rouyer, A. Santamarina, "Criticality experiments for criticality codes validation on low-moderate MOX media with Appareillage-B and EOLE," OCDE-WPNCs, Prague, 31 Aug 2004.
5. "Evaluation of Proposed Integral Critical Experiments with Low-Moderated MOX Fuels," *Final Report to the Nuclear Science Committee*, ISBN 92-64-01049-1, NEA No. 6047, OECD 2005.
6. T. Ivanova, V. Rouyer, Y. Rozhikhin, A. Tsiboulia, "Towards validation of criticality calculations for systems with MOX powders," *Annals of Nuclear Energy*, **36**, pp.305-309 (2009).
7. T. Ivanova et al., "OECD Expert Group on Uncertainty Analysis for Criticality Safety Assessment: Current activities," *Proc. of International Conf. PHYSOR2010*, Pittsburgh (USA), 9-14 May 2010.
8. *International Handbook of Evaluated Criticality Safety Benchmark Exp.*, NEA/NSC/DOC(95)03.
9. J.M Gomit et al., "CRISTAL criticality package twelve years later and new features," *Proc. of the International Conference of Nuclear Criticality Safety ICNC2011*, Edinburgh (UK), 19-23 Sept 2011.
10. A. Santamarina et al., "The JEFF-3.1.1 Nuclear Data Library," *JEFF Report 22*, OECD/NEA No.6807, edited by A. Santamarina, D. Bernard and Y. Rugama (2009).
11. R. Sanchez, "APOLLO2 Year 2010," *Nucl. Eng. & Technology*, **Vol 42 n°5**, pp.474-499 (2008).
12. A. Santamarina, V. Marotte, S. Misu, A. Sargeni, C. Vaglio, I. Zmijarevic, "Advanced neutronics tools for BWR design calculations," *Nucl. Eng. and Design*, **238**, pp.1965-1974 (2008).
13. N. Hfaiedh and A. Santamarina, "Determination of the Optimized SHEM Mesh for Neutron Transport Calculation," *Proc. Int. Conf. M&C2005*, Avignon (France), Sept 12-15, 2005.
14. J.-P. Both et al., "TRIPOLI4", *Proc. of Int. Conf. SNA '2003*, Paris (France), September 22-24 (2003).
15. A. Santamarina, "The JEFF3.1.1 Library for Accurate Criticality-Safety Calculations," *Proc. of the International Conference of Nuclear Criticality Safety ICNC2011*, Edinburgh (UK), 19-23 Sept 2011.
16. A. Santamarina, D. Bernard, P. Blaise, P. Leconte, J-M. Palau, B. Roque, C. Vaglio, J-F. Vidal, "Validation of the new code package APOLLO2.8 for accurate PWR neutronics calculations," *Proc. of the Int. Conf. M&C2013*, Sun Valley (USA), May 5-9, 2013.
17. C. Vénard, A. Santamarina, A. Leclainche, C. Mounier, "The R.I.B. Tool for the Determination of Computational Bias and Associated Uncertainty in the CRISTAL Criticality-Safety Package," *Proc. of NCSD 2009*, Richland (Washington), Sept 13-17, 2009, CD-ROM, ANS LaGrange Park, IL (2009).
18. C. Vénard, A. Santamarina, A. Coulaud, "Calculation Error and Uncertainty due to Nuclear Data. Application to MOX Fissile Media", *Proc. Conf. NCSD2005*, Knoxville (USA), Sept 19–22, 2005.
19. D. Cacuci, "Sensitivity and uncertainty analysis, vol 1" *Chapman & Hall/CRC Press*, (2003).
20. A. Santamarina, D. Bernard, N. Dos Santos, C. Vaglio, L. Leal, "Re-estimation of Nuclear Data and JEFF3.1.1 Uncertainty Calculation," *Proc. Int. Conf. PHYSOR2012*, Knoxville, April 15-20, 2012.
21. C. De Saint Jean et al., "Estimation of multi-group cross section covariances", *Proc. of Int. Conf. PHYSOR2012*, Knoxville (USA), April 15-20, 2012.
22. A. Santamarina, S. Cathalau, J.P. Chauvin, "Undermoderated PWR neutronic Qualification through the ERASME exp.," *Proc. Int. Top. Meeting Advances in Reactor Physics*, Paris, April 27-30, 1987.
23. L. N. Usachev, "Perturbation theory for the breeding ratio," *Journal of Nuclear Energy. Parts A/B. Reactor Science and Technology*, Volume **18**, Issue 10, pp. 571-583 (1964).